Double-Resonance Spectroscopy of Interacting Rydberg-Atom Systems

A. Reinhard, K. C. Younge, T. Cubel Liebisch,* B. Knuffman, P. R. Berman, and G. Raithel

FOCUS Center and Michigan Center for Theoretical Physics, Department of Physics, University of Michigan, Ann Arbor, Michigan 48109, USA

(Received 29 November 2007; published 13 June 2008)

The energy level spectrum of a many-body system containing two shared, collective Rydberg excitations is measured using cold atoms in an optical dipole trap. Two pairs of independently tunable laser pulses are employed to spectroscopically probe the spectrum in a double-resonance excitation scheme. Depending on the magnitude of an applied electric field, the Rydberg-atom interactions can vary from resonant dipole-dipole to attractive or repulsive van der Waals, leading to characteristic signatures in the measured spectra. Our results agree with theoretical estimates of the magnitude and sign of the interactions.

DOI: 10.1103/PhysRevLett.100.233201 PACS numbers: 34.20.Cf, 03.67.−a, 32.70.Jz, 32.80.Ee

Systems of cold Rydberg atoms provide an excellent platform for the study of many-body, collective phenomena. For example, Rydberg-atom systems closely resemble certain condensed matter physics systems such as spin glasses and amorphous solids [1,2]; they may spontaneously evolve into novel states of matter such as ultracold plasmas [3,4] and may undergo quantum diffusion processes [1,2,5,6]. When an ensemble of cold atoms is excited into Rydberg states, the excitations can be shared collectively among all atoms within certain regions. This situation is analogous to delocalized Mott-Wannier excitons in crystals. The analogy between atomic systems and excitons is strengthened by the recent observation of Bose-Einstein condensation of excitons [7]. Rydberg atoms also have applications in neutral-atom quantum information processing schemes that rely on the interaction among Rydberg atoms to perform a gate operation [8–10].

In connection with quantum information schemes, there has been considerable interest in demonstrating a dipole blockade involving collective Rydberg excitations. In a fully blockaded system, optical fields resonantly coupling the ground state to a Rydberg level can generate at most one collective Rydberg excitation; successive excitations are unlikely to occur because they are shifted out of resonance due to the strong electrostatic interactions between Rydberg atoms. Evidence for excitation blockades has been provided in a number of independent experiments, in which reduced excitation rates [11–13] and a narrowing of the counting statistics of the excited Rydberg populations [14] were observed. However, to our knowledge, there has been no direct spectroscopic proof that the blockade mechanism is operative. Such proof would require one to show that the excitation to the collective state involving two Rydberg excitations occurs at a transition frequency that differs from that of the first excitation.

We use optical excitation pulses to probe the first two steps of the Rydberg-excitation ladder and so provide spectroscopic proof of the blockade mechanism. The energy level scheme is illustrated schematically in Fig. 1, where $|kr\rangle$ denotes a system with k shared Rydberg excitations. The $|0r\rangle \rightarrow |1r\rangle$ transition is not shifted by Rydberg-Rydberg interactions, since there is at most one Rydberg excitation in the system. However, such interactions play a critical role in the $|1r\rangle \rightarrow |2r\rangle$ transition, because in this case the target state has two Rydberg excitations. In the states $|2r\rangle$, the electrostatic interaction between Rydberg atoms results in an R^{-3} interatomic potential in the case of a resonant dipole-dipole (d-d) interaction and an R^{-6} interatomic potential in the case of an off-resonant van der Waals (vdW) interaction. The specific nature of the interaction can be changed by the application of an external static electric field. The states $|2r\rangle$ are shifted due to these interactions and form a *band* of energies, as shown in Fig. 1, because the excitations are coherently shared among atoms separated by a range of different distances. For the d-d interaction, there are two bands of levels symmetrically placed above and below the value $2W$ (where W is the single Rydberg-excitation energy) [9]. For the vdW interaction (which may be positive or negative), there is a single band of levels shifted by the

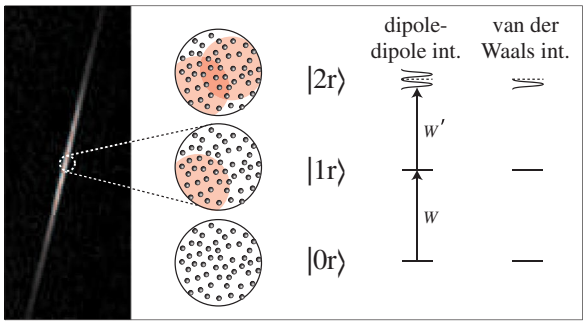

FIG. 1 (color online). The left panel shows a shadow image of atoms in an optical dipole trap. The right panel shows an excitation domain [23] with zero, one, or two interacting Rydberg excitations. The nature of the energy-shifted band of states $|2r\rangle$ depends on whether the interactions are resonant dipole-dipole or van der Waals in nature. Owing to the interactions, the $|1r\rangle \rightarrow |2r\rangle$ transition energy W' differs from the energy of a single Rydberg excitation W.

vdW interaction strengths [15]. In our experiment, a first set of laser pulses is employed to resonantly excite the state $|1r\rangle$, and a second set of pulses is used to map out the energy bands associated with the states $|2r\rangle$.

An optical dipole trap, formed by focusing a 5 W, 1064 nm laser beam through a magneto-optical trap (MOT), is used to prepare dense clouds of ^{85}Rb atoms. The dipole trap is loaded by overlapping the 1064 nm light and the MOT trapping light in time for 30 ms. The MOT trapping light is then switched off, and all atoms not trapped in the focus of the 1064 nm beam are allowed 38 ms to fall out of the trapping region. By using this procedure, we achieve cigar-shaped atomic distributions having a full width at half maximum (FWHM) diameter of 16 μm, central density $\approx 4 \times 10^{11}$ cm^{-3}, atom number $\approx 3 \times 10^4$, and temperature ≈ 1 mK, as determined by shadow imaging. A shadow image of a typical dipole trap is shown in Fig. 1. To avoid the effect of light shifts on the Rydberg transition, the dipole trap beam is switched off before the atom sample is optically excited into Rydberg levels.

To create Rydberg excitations, we use coincident, counterpropagating, ≈ 2 MHz linewidth, resonant laser pulses to drive the two-photon transition $5S_{1/2} \rightarrow 5P_{3/2} \rightarrow nD_{5/2}$, where n is the principal quantum number of the target Rydberg state. The lower-transition (780 nm) pulse is characterized by an intensity distribution having a FWHM of about 3 mm and a peak Rabi frequency of 3.5 MHz, as determined by Autler-Townes spectroscopy [16]. The upper-transition (480 nm) pulse is focused to an intensity FWHM of 19 μm, approximately the diameter of the atom distribution. The Rabi frequency on the upper transition is estimated to be ~ 3 MHz. The beam driving the upper transition is derived from a frequency-doubled, 960 nm diode laser (Toptica DL-100) which is locked to a pressure-tuned Fabry-Perot cavity [17]. The optical pulses have a temporal FWHM of the intensity distribution of 100 ns. Several hundred nanoseconds following the optical pulses, the number of Rydberg excitations and the Rydberg-state distribution are determined by using state-selective field ionization (SSFI) and a microchannel-plate detector [18].

In a first set of experiments, we excite atoms to $45D_{5/2}$ states without and with an electric field. In zero applied field, the level shifts of the states $|2r\rangle$ are negative and primarily vdW in character [15]. The resonant d-d case, in which the band of states $|2r\rangle$ is symmetrically split, is realized by tuning the transition

$$45D_{5/2} + 45D_{5/2} \rightarrow 43F_{7/2} + 47P_{3/2} \qquad (1)$$

into resonance by using an applied electric field. To determine the resonant electric field E_F at which this Förster resonance occurs, we examine SSFI signals as a function of applied electric field, similar to the method used in Ref. [19]. The fraction of the FI signal in the product states $47P$ and $43F$ becomes strongly enhanced as the infinite-separation energy defect of the transition in Eq. (1) approaches zero [20]. In Fig. 2(a), we show a series of SSFI signals for excitation into the $45D_{5/2}$ state for the indicated values of the applied electric field. The fraction of the FI signal in $47P$ and $43F$ states clearly depends on the applied electric field. In Fig. 2(c), we plot the fraction of the FI spectrum in $47P$ states as a function of the applied electric field and determine the resonant field $E_F = 0.23$ V/cm. This value is somewhat lower than the calculated values of Förster-resonance fields, 0.26, 0.28, and 0.36 V/cm [15], which are expected to merge into a single signature in the experiment, as seen in Fig. 2(c). Stray electric fields may cause the discrepancy between experimental and theoretical Förster-resonance fields. In the following, we use the electric fields $E = 0$ and $E = E_F$ to study Rydberg-excitation spectra for vdW and d-d interactions, respectively.

To measure the spectra of the transitions $|0r\rangle \rightarrow |1r\rangle$ and $|1r\rangle \rightarrow |2r\rangle$ in Fig. 1, we apply two pairs of optical pulses, labeled as "first pulses" and "second pulses" in the timing diagram shown in Fig. 3. The two pairs of pulses are separated by 400 ns in time, which is the lower limit set by the frequency switching time of the utilized acousto-optic modulators (AOM). Each pair of pulses contains a 780 nm pulse and a coincident 480 nm pulse, which we refer to as the lower-transition and upper-transition [21] pulses, respectively. The lower-transition pulses are always resonant with the $5S_{1/2} \rightarrow 5P_{3/2}$ transition. The frequency of the first upper-transition pulse ν_1 is resonant with the interaction-free transition energy $5P_{3/2} \rightarrow 45D_{5/2}$, while the frequency of the second upper-transition pulse ν_2 is scanned in 4 MHz steps about ν_1 by using an AOM. The first pair of pulses primarily drives the $|0r\rangle \rightarrow |1r\rangle$ transi-

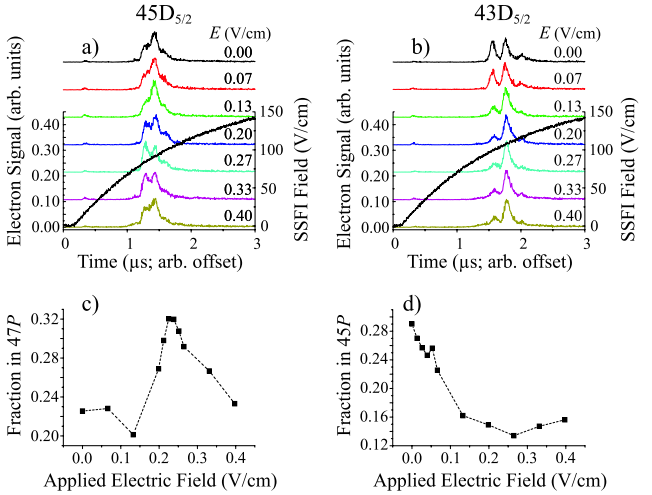

FIG. 2 (color online). Effect of an applied electric field E on state-mixing collisions for excitation into the states $45D_{5/2}$ (a),(c) and $43D_{5/2}$ (b),(d). (a) and (b) show SSFI signals after 700 ns interaction time for different values of E along with the SSFI electric field pulse. (c) and (d) show the fraction of the total SSFI signal in $47P$ or $45P$ states as a function of E.

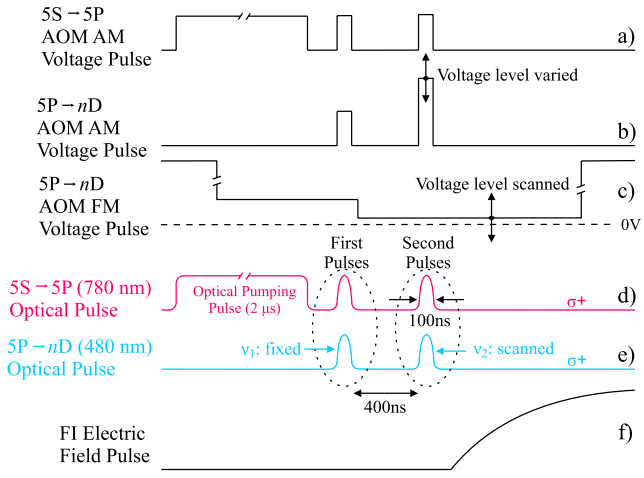

FIG. 3 (color online). Experimental timing diagram. (a)–(c) Control voltages applied to the acousto-optic modulators to generate the optical pulses shown in (d) and (e). (f) SSFI pulse.

tion shown in Fig. 1. The second pair of pulses is used to probe the energy shifts of the states $|2r\rangle$ as the frequency ν_2 is scanned.

In the experiment, it is essential to have a second upper-transition pulse (with frequency ν_2) of the same intensity as the first upper-transition pulse (with frequency ν_1). However, as the frequency ν_2 is scanned, there are unavoidable intensity variations that result from the frequency response of the optical system (AOM and fiber). We remedy this problem by actively controlling the intensity of the second pulse with a feedback scheme that utilizes the amplitude-modulation capability of the AOM.

To characterize the band structure of the states $|2r\rangle$, we record the number of Rydberg excitations produced as we vary ν_2 for three cases: only the first pair of pulses on, only the second pair on, and both pairs on [henceforth referred to as S_1, $S_2(\nu_2)$, and $S_{1+2}(\nu_2)$, respectively]. The value of S_1 is approximately constant because ν_1 is fixed. We are interested only in its average, denoted as $\bar{S}_1$. The spectrum $S_2(\nu_2)$ corresponds to the transition $|0r\rangle \rightarrow |1r\rangle$ in Fig. 1. Since the first pair of pulses is resonant with the transition $|0r\rangle \rightarrow |1r\rangle$, $\bar{S}_1$ is equal to the peak value of $S_2(\nu_2)$. The spectrum $S_{1+2}(\nu_2)$ results from the combined effect of two pulse pairs: The first pair of pulses drives the transition $|0r\rangle \rightarrow |1r\rangle$ and contributes the constant offset $\bar{S}_1$ to the signal, while the second pair of pulses may also drive the transition $|1r\rangle \rightarrow |2r\rangle$. Since we are interested primarily in the number of Rydberg counts added by the second set of pulses, in the following we display the spectra $\tilde{S}_{1+2}(\nu_2) \equiv S_{1+2}(\nu_2) - \bar{S}_1$. We compare $\tilde{S}_{1+2}(\nu_2)$ with $S_2(\nu_2)$ to determine how the Rydberg-Rydberg interactions modify the spectrum of the transition $|1r\rangle \rightarrow |2r\rangle$ from the spectrum of the interaction-free transition $|0r\rangle \rightarrow |1r\rangle$.

In Figs. 4(a) and 4(b), we display $\tilde{S}_{1+2}(\nu_2)$ (circles; right axis) along with $S_2(\nu_2)$ (squares; left axis) for excitation into $45D_{5/2}$ states. Figures 4(a) and 4(b) show the spectra for zero applied field and an applied field of E_F, respectively. Based on the number of detected Rydberg excitations (~10 in Fig. 4), an estimated single-domain excitation efficiency of about 50%, and the SSFI electron detection efficiency (~50%), we estimate that our excitation volume (16 μm × 16 μm × 19 μm) contains of order 40 excitation domains of the type sketched in Fig. 1. The two spectra $\tilde{S}_{1+2}(\nu_2)$ demonstrate the difference in the nature of the energy shift of states $|2r\rangle$ for vdW (off-resonant) and d-d (resonant) interactions. The zero-field spectrum $\tilde{S}_{1+2}(\nu_2)$ in Fig. 4(a) exhibits a wing on the negative side of $\nu_2 - \nu_1$, providing evidence for a band of $|2r\rangle$-excitation frequencies shifted to the low-frequency side of ν_1. This observation is consistent with calculations showing that in zero applied field the interactions among $45D_{5/2}$ atoms are negative (attractive) and primarily vdW in nature [15]. The spectrum $\tilde{S}_{1+2}(\nu_2)$ in Fig. 4(b), taken with the applied electric field E_F, exhibits symmetric wings, providing evidence for two bands of $|2r\rangle$-excitation frequencies symmetrically located about ν_1. This is consistent with the effect of a Förster resonance on the spectrum of the doubly excited states $|2r\rangle$ [9]. We note that the spectra $S_2(\nu_2)$ are not broadened in a manner resembling the structures seen in $\tilde{S}_{1+2}(\nu_2)$. Therefore, the signal in the wings of $\tilde{S}_{1+2}(\nu_2)$ cannot be significantly affected by two-photon excitation $|0r\rangle \rightarrow |2r\rangle$; it must be due to sequential excitation $|0r\rangle \rightarrow |1r\rangle \rightarrow |2r\rangle$.

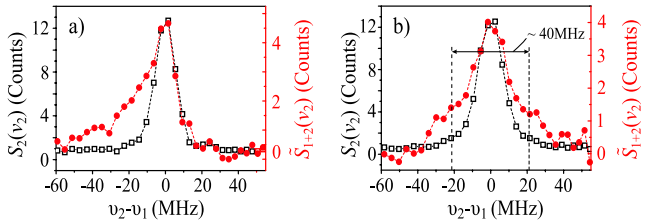

FIG. 4 (color online). Spectra for excitation into the $45D_{5/2}$ state: $S_2(\nu_2)$ (squares; left axes), $\tilde{S}_{1+2}(\nu_2)$ (circles; right axis). (a) shows data with zero applied electric field and 240 averages per point, while (b) shows data with an applied field of E_F and 200 averages per point.

It is important to note that the first set of laser pulses excites only a fraction of all excitation domains from the state $|0r\rangle$ to the state $|1r\rangle$. To minimize power broadening of the $|0r\rangle \rightarrow |1r\rangle$ transition, we limit the Rabi frequencies of the lower- and upper-transition pulses to $\Omega_{5S\rightarrow 5P} = 3.5$ MHz and $\Omega_{5P\rightarrow nD} \sim 3$ MHz, resulting in less than optimal excitation efficiency. Therefore, the action of the second pair of laser pulses is twofold: Excitation domains left in $|0r\rangle$ after the first pulses are driven on the transition $|0r\rangle \rightarrow |1r\rangle$, while excitation domains left in $|1r\rangle$ after the first set of laser pulses are driven on the transition $|1r\rangle \rightarrow |2r\rangle$. As a result, the spectra $\tilde{S}_{1+2}(\nu_2)$ in Figs. 4(a) and 4(b) are a weighted sum of $S_2(\nu_2)$, shown in the same panels, and the spectrum of the transition $|1r\rangle \rightarrow |2r\rangle$. In particular, we expect that the excitations in $\tilde{S}_{1+2}(\nu_2)$ at $\nu_2 - \nu_1 = 0$ are due to unexcited domains being driven on the tran-

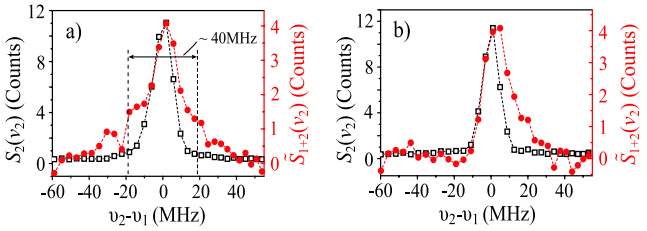

FIG. 5 (color online). Spectra for excitation into the $43D_{5/2}$ state: $S_2(\nu_2)$ (squares; left axis) and $\tilde{S}_{1+2}(\nu_2)$ (circles; right axis). (a) shows data with zero applied electric field and 455 averages per point, while (b) shows data with an applied field of 0.15 V/cm and 260 averages per point.

sition $|0r\rangle \rightarrow |1r\rangle$ by the second pair of pulses. To extract the $|1r\rangle \rightarrow |2r\rangle$ component of $\tilde{S}_{1+2}(\nu_2)$, one may subtract $\alpha S_2(\nu_2)$ from $\tilde{S}_{1+2}(\nu_2)$, where α is a weighting factor <1. This procedure yields $|1r\rangle \rightarrow |2r\rangle$ spectra that feature a redshifted peak for Fig. 4(a) and two symmetric peaks for Fig. 4(b), as sketched in Fig. 1. Since the proper value of α is unknown, we do not present detailed results of this procedure.

The sign of the vdW shift can be changed between attractive and repulsive by choosing appropriate quantum states and/or applied electric fields. In Figs. 2(b) and 2(d), we show averaged SSFI signals for laser excitation into $43D_{5/2}$ states and the fractions of the SSFI signals in $45P$ states for a range of applied electric fields, respectively. The data show that a Förster resonance exists for $43D_{5/2}$ near zero applied electric field; this resonance is due to the channel $43D_{5/2} + 43D_{5/2} \rightarrow 41F_{7/2} + 45P_{3/2}$ [15]. In zero electric field, the infinite-separation energy defect of this channel is only -8 MHz (product states lower in energy) [20]. The channel becomes more off-resonant as an electric field is applied, changing the character of the interaction to van der Waals. A perturbative calculation of the interaction energy, identical to those carried out in Ref. [15], shows that the van der Waals shifts are positive (i.e., repulsive interactions) for electric fields in the range 0.1–0.45 V/cm. Thus, in the spectra $\tilde{S}_{1+2}(\nu_2)$, we expect to observe evidence for two bands of $|2r\rangle$-excitation frequencies symmetrically located about ν_1 with zero applied electric field and for a single, blueshifted band with an applied field in the above range. Measurements of the spectra $S_2(\nu_2)$ and $\tilde{S}_{1+2}(\nu_2)$ for $43D_{5/2}$ atoms in zero electric field and in an applied electric field of 0.15 V/cm, shown in Fig. 5, are consistent with these expectations.

We show finally that the magnitudes of the frequency displacements of $|2r\rangle$ observed here are in agreement with theoretical predictions for d-d interactions presented in Ref. [9]. Figure 2(a) of Ref. [9] shows the calculated band structure of the states $|2r\rangle$ for the case of an exact Förster resonance [22]. We connect this figure with our data by setting the ensemble volume V defined in Ref. [9] equal to the volume of one excitation domain in our experiment. The volume of one excitation domain is estimated by dividing the excitation volume by the number of excitation domains ($\sim$40, as estimated above). By using this volume and Fig. 2(a) of Ref. [9], we calculate that, in the d-d case, the bands of states $|2r\rangle$ should peak at about $\nu_2 - \nu_1 \approx \pm 20$ MHz. This value agrees with the band splittings that can be estimated from our data [see arrows in Figs. 4(b) and 5(a)].

In conclusion, we have measured the energy band structure of a many-body system containing two shared Rydberg excitations. Depending on the magnitude of an applied electric field, the band structure reflects either symmetric dipole-dipole or attractive or repulsive van der Waals interactions. The magnitude and sign of the observed energy shifts agree with theory. In the future, we plan to use the same technique to study the interaction of Rydberg excitations prepared in optical dipole traps at well-defined, variable separations. Such measurements will be important within the context of neutral-atom quantum computation [8,9].

This work was supported in part by NSF Grants No. PHY-0114336, No. PHY-0555520, and No. PHY-0244841.

*Present address: NIST Time and Frequency Division, 325 Broadway, Boulder, CO 80305, USA.

[1] W. R. Anderson *et al.*, Phys. Rev. Lett. **80**, 249 (1998).
[2] I. Mourachko *et al.*, Phys. Rev. Lett. **80**, 253 (1998).
[3] T. C. Killian *et al.*, Phys. Rev. Lett. **83**, 4776 (1999).
[4] M. P. Robinson *et al.*, Phys. Rev. Lett. **85**, 4466 (2000).
[5] W. R. Anderson *et al.*, Phys. Rev. A **65**, 063404 (2002).
[6] M. Mudrich *et al.*, Phys. Rev. Lett. **95**, 233002 (2005).
[7] J. Kasprzak *et al.*, Nature (London) **443**, 409 (2006).
[8] D. Jaksch *et al.*, Phys. Rev. Lett. **85**, 2208 (2000).
[9] M. D. Lukin *et al.*, Phys. Rev. Lett. **87**, 037901 (2001).
[10] M. Saffman and T. G. Walker, Phys. Rev. A **72**, 022347 (2005).
[11] D. Tong *et al.*, Phys. Rev. Lett. **93**, 063001 (2004).
[12] T. Vogt *et al.*, Phys. Rev. Lett. **97**, 083003 (2006).
[13] T. Vogt *et al.*, Phys. Rev. Lett. **99**, 073002 (2007).
[14] T. Cubel Liebisch *et al.*, Phys. Rev. Lett. **95**, 253002 (2005).
[15] A. Reinhard *et al.*, Phys. Rev. A **75**, 032712 (2007).
[16] B. K. Teo *et al.*, Phys. Rev. A **68**, 053407 (2003).
[17] E. Hansis, Rev. Sci. Instrum. **76**, 033105 (2005).
[18] J.-H. Choi *et al.*, Adv. At. Mol. Opt. Phys. **54**, 131 (2007).
[19] A. L. de Oliveira *et al.*, Phys. Rev. Lett. **90**, 143002 (2003).
[20] A. Reinhard *et al.*, Phys. Rev. Lett. **100**, 123007 (2008).
[21] These are not to be confused with the $|0r\rangle \rightarrow |1r\rangle$ and $|1r\rangle \rightarrow |2r\rangle$ transitions in Fig. 1.
[22] The case of vdW interactions is not treated in this reference.
[23] An "excitation domain" is a spherical volume with radius r_{ed} such that the energy shift of two atoms separated by $2r_{ed}$ equals the laser linewidth.